ISSN 2347-3487

An analysis of the transport properties and mechanical stability of rapidly solidified Al-Sb alloy

Mustafa Kamal[1], Abu-Bakr El-Bediwi[1], Rizk Mostafa Shalaby[1,*] and Qutaiba Rasheed Solaiman[1,2]

[1] Metal Physics Lab., Physics Department, Faculty of Science, Mansoura University, Mansoura, Egypt.

*doctorrizk2@yahoo.co.uk

[2] On leave, M.Sc. student, Iraq

Abstract

The structure of a series of AlSb alloys prepared by melt spinning have been studied in the as melt–spun ribbons as a function of antimony content .The stability of these structures has been related to that of the transport and mechanical properties of the alloy ribbons. Microstructural analysis was performed and it was found that only Al and AlSb phases formed for different composition. The electrical, thermal and the stability of the mechanical properties are related indirectly through the influence of the antimony content. The results are interpreted in terms of the phase change occurring to alloy system. Electrical resistivity, thermal conductivity, elastic moduli and the values of micro hardness are found to be more sensitive than the internal friction to the phase changes.

Keywords

Transport properties; Mechanical properties; Microstructure; Al-Sb alloys

Council for Innovative Research

Peer Review Research Publishing System

Journal: JOURNAL OF ADVANCES IN PHYSICS

Vol. 10, No. 2

www.cirjap.com, japeditor@gmail.com

ISSN 2347-3487

1. Introduction

It is well known that the structure and physical properties of Al-Sb binary alloys rapidly solidified from the molten state are influenced by several parameters such as antimony content, number of atoms per unit cell, lattice disorder ,particle size and the amount of aluminium antimonied (AlSb)formed in the melt-spun ribbons of Al_{100-x}-Sb_x where($x \geq$ 2wt%Sb).These parameters have not investigated, we hope to report some interpretations, which are primarily aimed at these aspects .To date ,however, indefinite number of studies have been made on the structure and physical properties of rapid quenched ribbons Al-Sb alloys [1]. In addition on what has been reported, Al and Sb resources abound on the earth and the method of their manufacturing and use is environmentally friendly. So aluminuim antimonide AlSb is one of a series of III-V compound semiconductor with zinc blende structure as show in (Fig 1), and it has a good potential application for solar cells with an indirect band gap is 1.7eV at room temperature [2,3].

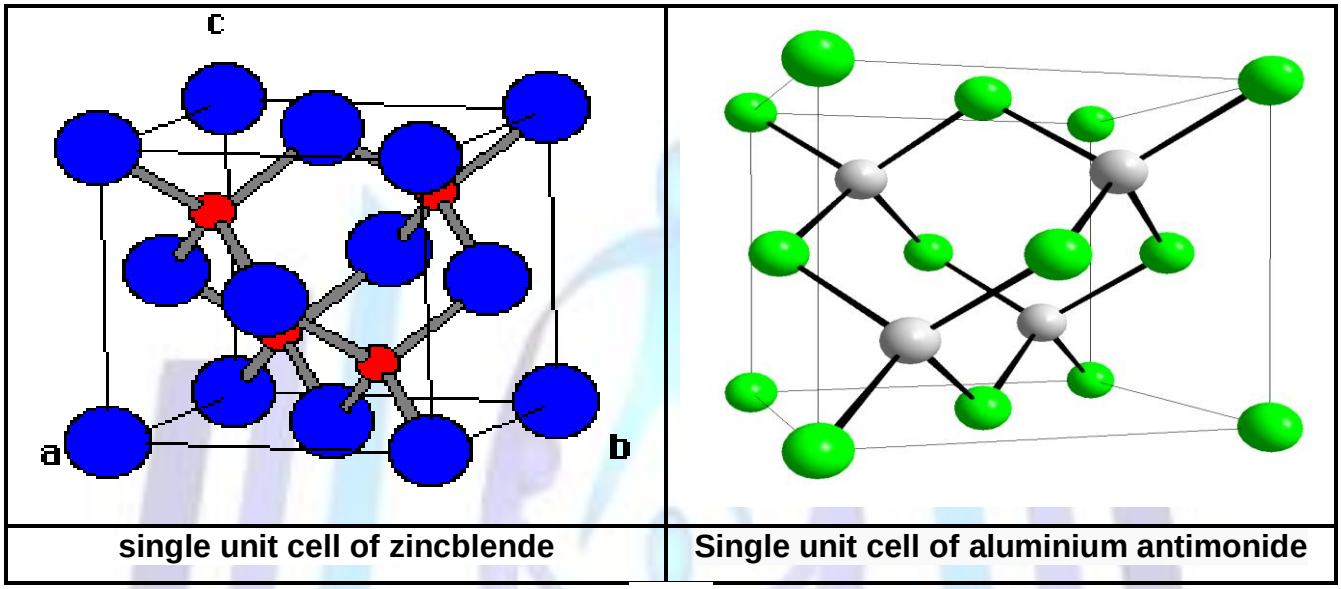

single unit cell of zincblende | Single unit cell of aluminium antimonide

Fig. 1

Aluminium antimonide (AlSb) has been investigated as a candidate for several electronic and optoelectronic applications [4]. The early history of assessment of the Al-Sb system by Gautier [5] and by Combell and Mathews [6], the liquidus curves obtained by solidification experiments exhibited two peaks, one at antimony, Sb and one at the AlSb compound [7]. M.kamal and Shaban investigated structure –property of rapidly quenched aluminium-antimony alloys before and after gamma irradiation [8,9]. Tron Arne Nilson et al [10] was determined the lattice constant of AlSb, it was found to be 6.1361Å which is in agreement with earlier published results by Giesecke and Pfister[11]. The temperature dependent lattice constant was found to be different from linear extrapolation of Madelung [12] and Vurgaftman et al [13] results. The present work aims to carry out structural observations of the rapidly quenched spun ribbons Al_{100-x} - Sb_x where ($x \geq$ 2wt%Sb). The detailed research on melt – quenched ribbons from molten state has been done. The effect of antimony content on the physical properties has been studied. The electrical, thermal and mechanical properties of Al-Sb melt – spun ribbons have been investigated. In this paper, the results are provided with the structure of several Al-Sb rapidly solidified from melt for a wide range of antimony content. Moreover Al-Sb phases exhibit a simple phase diagram (Fig 2) with two eutectic points and an intermediate line compound of Al-Sb [14]. Composition and properties of the system investigated are shown in table (1).

ISSN 2347-3487

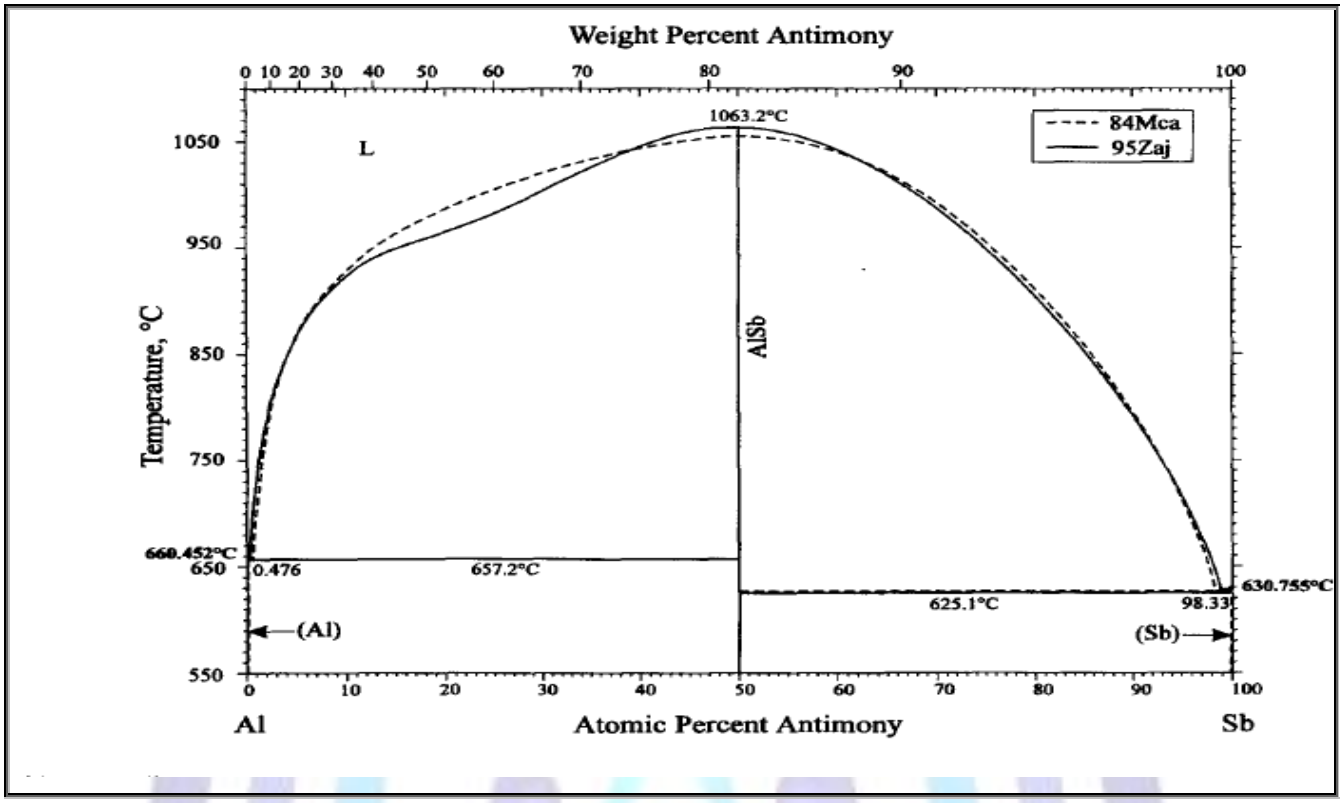

Fig. 2: Al-Sb phase diagram

Table 1 : XRD details of Al-Sb melt spun alloys

System wt%	Density g/cm^3	V(Å^3) Al	particle size (Å^3) Al	V(Å^3) AlSb	particle size(Å^3) AlSb
Al pure	2.35	67.79	374.97		
Al-2wt%Sb	2.05	66.63	353.2		
Al-5wt%Sb	2.29	60.7	365.07	231.85	217.5
Al-7wt%Sb	2.1	66.63	350.68	230.69	436.2
Al-10wt%Sb	2.85	66.44	404.3	217.04	175.1
Al-12wt%Sb	2.5	66.68	401.4	231.74	465.3
Al-15wt%Sb	2.66	66.98	315.2	231.22	248.3
Al-17wt%Sb	2.14	66.52	400.7	230.29	202.3
Al-20wt%Sb	2.64	66.66	360.09	204.2	231.37
Al-25wt%Sb	2.87	66.79	354.06	229.75	271.21
Al-33wt%Sb	2.05	66.73	478.5	232.4	149.1
Al-50wt%Sb	2.77	66.62	403.19	229.75	219.47
Al-67wt%Sb	2.615	66.74	333.97	220	262.42

2. Experimental

Elemental Al(99.9% purity) and Sb (99.9% purity) were used to prepare the alloy of nominal composition Al_{100-x}-Sb_x($x \geq$ 2wt%Sb). The charges were melted in a nuclear graphite crucible using an electric furnace and were cast in to ingots in a graphite chill mold. Using a single roller melt spinning apparatus[15], the pre-alloyed ingots were remelted by a

ISSN 2347-3487

muffle furnace in a crucible and then melt – spun on a copper roller with a diameter(0.2m) at a speed of revolutions per minute (rpm) giving a circumferential speed about 30.4ms^{-1} .The melt – spun ribbons obtained were typically (50-120μm in thickness and 3-5mm in width). The experimental technique utilized have been described in details [16,17] and will be repeated here only briefly. The investigated samples in the present work are Al_{100-x}-Sb_x where[x$\geq$2wt%Sb] were melted in a muffle furnace using aluminium and antimony of purity better 99.9%. The resulting alloys were curved and re-melted to increase the homogeneity.

From these ingots long ribbons of about 40mm, width 4mm and thickness about 0.009mm it was prepared by melt – spinning technique [15]. Phase identification was performed using x-ray diffraction (XRD) with Cu kα radiation. The micro-structural characterization was performed with **(**JEOL JSM-6510LV Low Vacuum, SEM and EDX) Scanning Electron Microscope (SEM). In situ electrical resistivity measurements have been carry out using the double-bridge technique` were measured using a Beckman industrial TP 850 digital thermometer. The elastic moduli, the internal friction, and the thermal diffusivity of melt-spun ribbons were tested in air a modified dynamic resonance technique [18]. The hardness of the quenched ribbons was calculated by using a digital Vickers micro hardness tester (model FM-7). By applying a load of 10 gf for 5sec via a Vickers diamond pyramid. More than fifteen indents were made on each sample to bring out any hardness variation due to presence of more phases, with one phase soft and ductile and another phase [19, 20]. The material flow rate Q_f has been empirically found to be an important chill block melt-spinning process variable and its dependence on readily adjustable apparatus parameters has been described by Liebermann [21, 22]. Much harder, so that the average value Hv would be obtained

In the present study this parameter is calculated from

$$Qf = VrW\,t \qquad (1)$$

Where Vr is the ribbon or substrate velocity, w is the ribbon width and t the average thickness calculated by dividing the ribbon mass by length density ρ and width w

$$t = \frac{m}{lw\rho} \qquad (2)$$

3. Results and discussions

3.1. Phase Identification

X-ray diffraction (XRD) analysis is applied to obtain information about crystalline matter on the atomic measure. The typical investigated parameters are the size and symmetry of the elementary cell, positions of individual atoms within the incipient cell and atomic vibration [23]. A chart of x-ray diffraction patterns is shown in Fig 3(a-m).The diffraction lines in the chart could be grouped into those from the face centered cubic structure of α-Al-phase, and those from the cubic structure of aluminium antimonide AlSb intermetallic compound. The phases in the melt – spun ribbons Al_{100-x}-Sb_x are the α-Al solid solution and the AlSb intermetallic compound. The phases were also identified by x-ray diffraction patterns at different compositions as indicated in the fig-3. The Sb-phase peaks appear simultaneously in the melt – spun ribbons, which demonstrate the coexistence of AlSb and Sb phases. The existence of Sb propose that a part of Sb and Al did not sufficiently combine to shape AlSb .The results of Jianxiong et al [3] reported that a part of Sb and Al did not sufficiently combine to form AlSb due to then uneven distributions in the multilayer films.

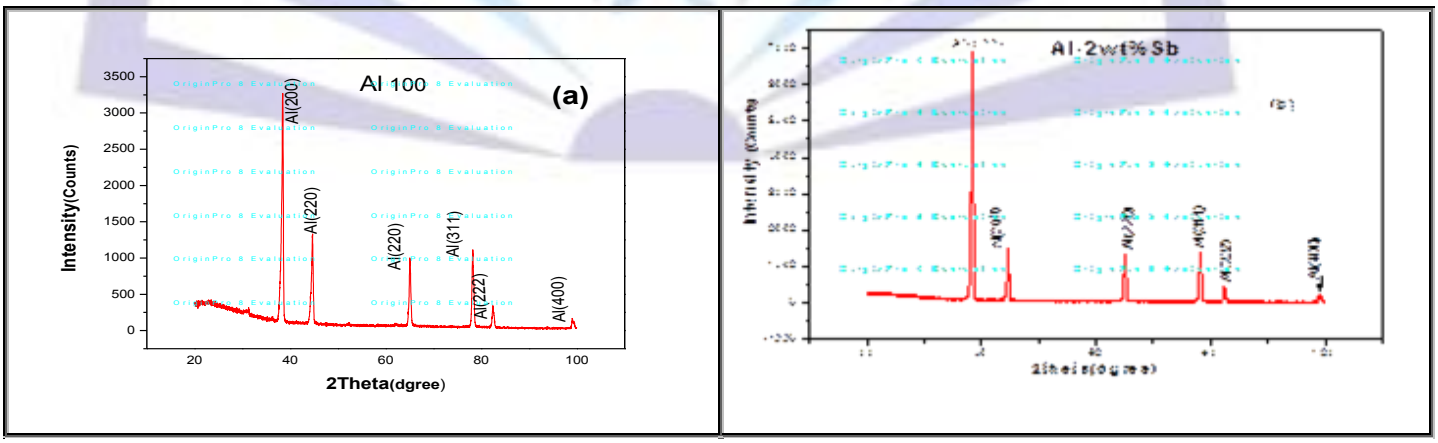

ISSN 2347-3487

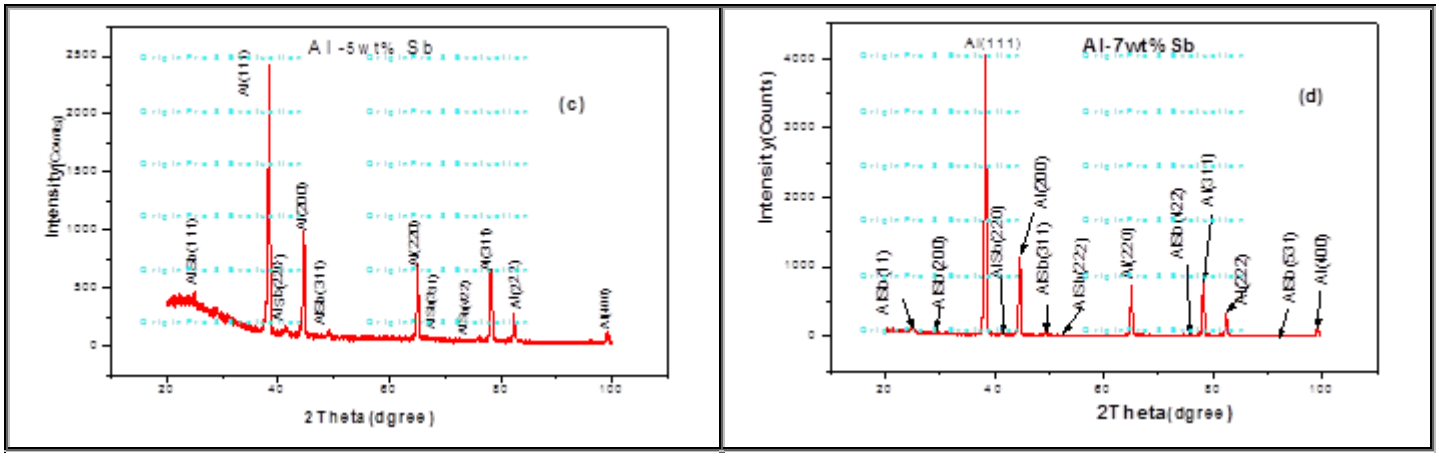

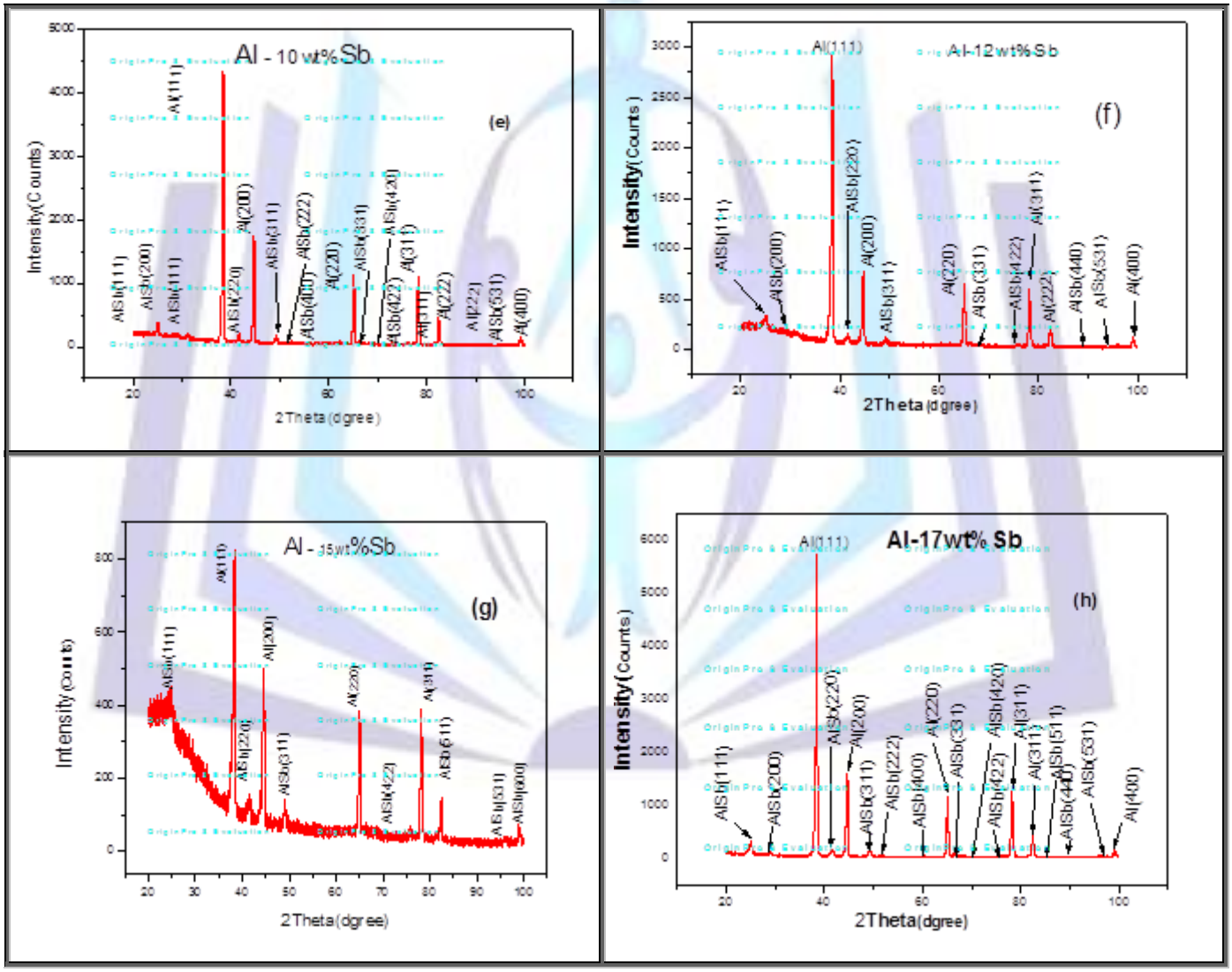

ISSN 2347-3487

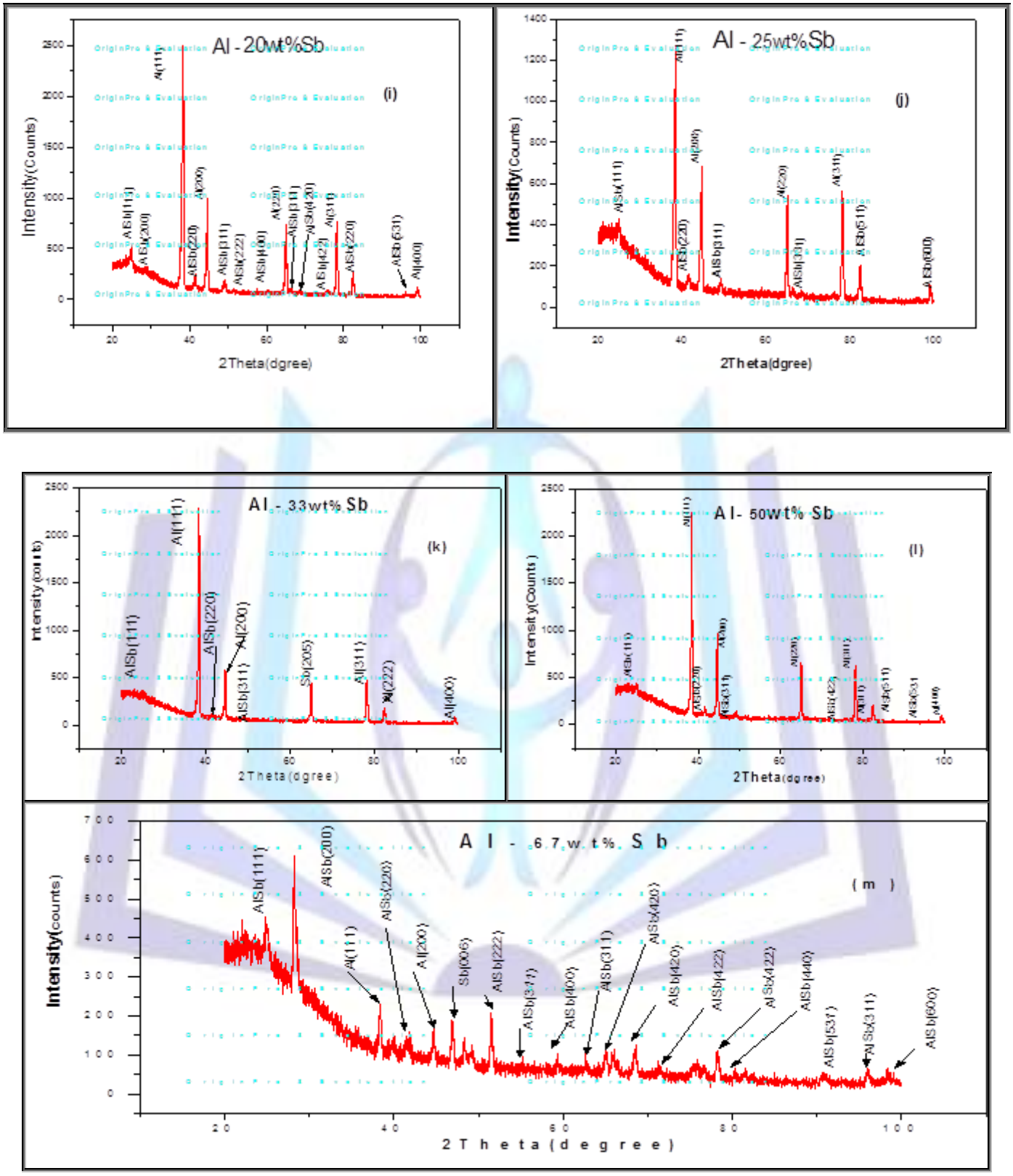

Fig. 3: XRD patterns of the melt – spun Al_{100-x}-Sb_x($x \geq$ 2wt%Sb)

The lattice parameter was determined from each peak and an average value was calculated. Table (2) shows the variation of lattice parameters versus Sb concentration for the aluminium-rich face centered cubic phases. Lattice parameter lowering up to about 5wt%Sb indicating that about 5wt%Sb can be retained in the Al-rich fcc phase by liquid –quenching. The lattice parameter of the cubic AlSb phase in these quenched ribbons was the same as that aluminium antimonide (AlSb) semiconductor [25-27] The size of the grains in a polycrystalline melt-spun metal alloy ribbons has pronounced effects on many of its properties. When the size of the individual crystals is less than approximately 1000Å in size

ISSN 2347-3487

appreciable broadening in the x-ray diffraction lines will occur. These regions may in fact correspond to the actual size of the particles. The extent of broadening of diffraction line is described by B, which is the full width of half maximum intensity of the peak (FWHM). After the value of B (in radians) is corrected for the instrumental contribution, it can be substituted in to Scherrer's equation:

$$B=\frac{0.9\lambda}{t\cos\theta} \qquad (3)$$

where t=diameter of crystal particle. The melt–spinning technique of metallic alloys has been shown to produce appreciable changes in the intensity distribution of diffracted x-rays. The most conspicuous of these effects are changes in line shape and in integrated intensity[21-24] Changes in integrated intensity have been studied and discussed by Hall and Williamson [28] and it is object of this section to interpret and correlate the changes in line shape with the simultaneous measurements of integrated intensity. Line width B, both FWHM and integral, were used in a Williamson–hall plot [29]. Usually, structural line expanding is split into crystallite size broadening and micro strain broadening [30]. Williamson - Hall plot was used as illustrated in fig 4 (a-m) , to deduce useful information, about the diameter of crystal particle (t) and the local lattice distortion$<\Sigma^2>$ in all phases in the melt –spun ribbons of Al-Sb alloys by the following relations

$$B = 1/t + 5 < \Sigma^2 >^{1/2} \frac{\sin\theta}{\lambda} \qquad (4)$$

where λ is a wave length and Θ is the angle of incidence of radiation

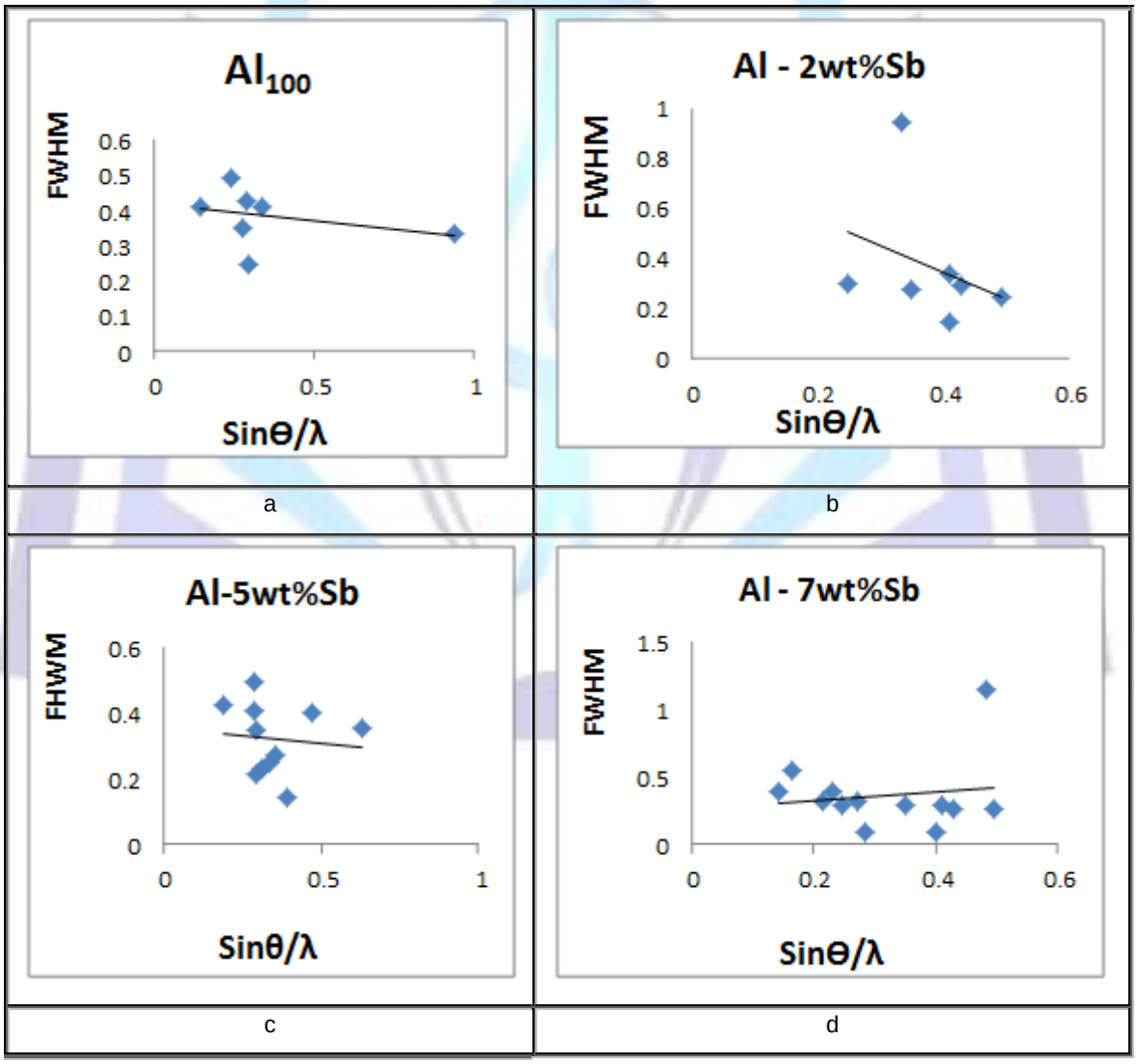

ISSN 2347-3487

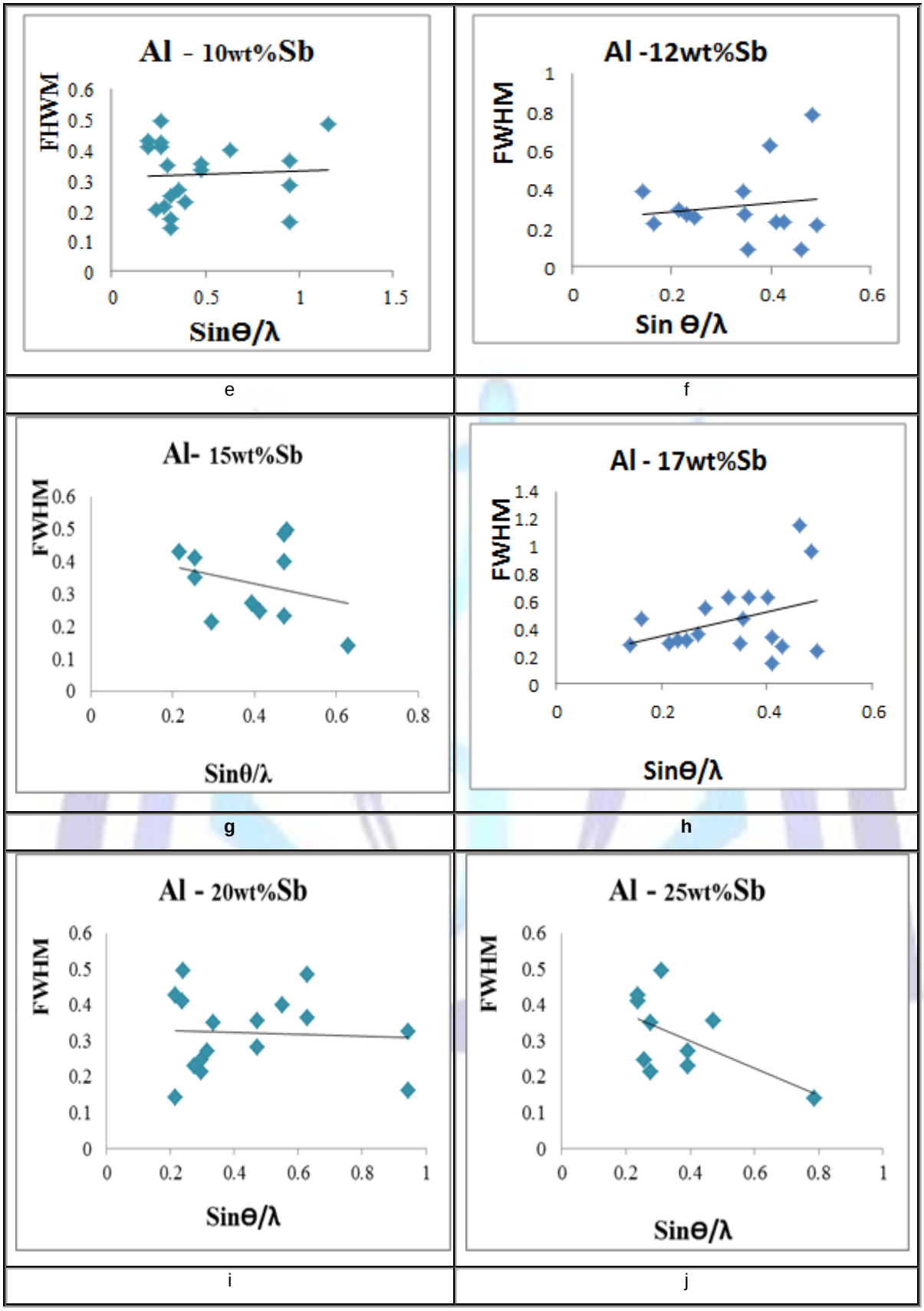

ISSN 2347-3487

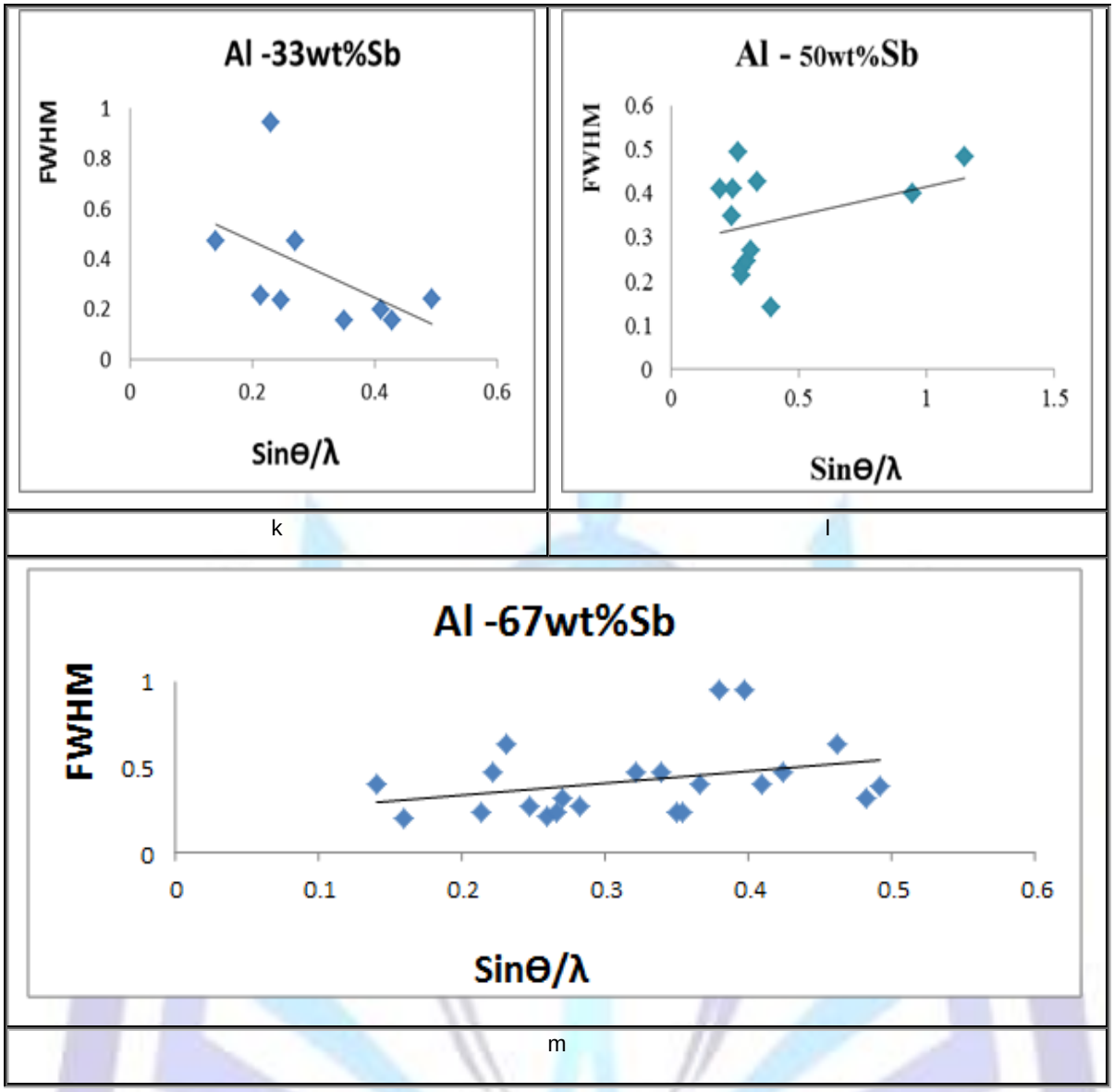

Fig. 4 .Williamson-Hall plot of FWHM values for Al_{100-x}-Sb_x($x \geq 2$wt%Sb)

The (1/t) and $5<\Sigma^2>^{1/2}$ parameters are given in table (2)

Table 2: Structural data for phases present in Al_{100-x} - Sb_x where($x \geq 2$wt%Sb) as quenched ribbons

System wt%	a(Å)		1/ t ($Å^{-1}$) $*10^{-3}$		$5<\Sigma^2>^{1/2}$	
	Al	AlSb	Al	AlSb	Al	AlSb
Al pure	4.08		3.7		1.43	
Al-2wt%Sb	4.05		2.95		1.27	
Al-5wt%Sb	3.93	6.14	2.92	4.78	1.19	2.05
Al-7wt%Sb	4.054	6.13	2.95	4.48	1.2	2.11
Al-10wt%Sb	4.05	6	2.6	6.76	1.06	2.91
Al-12wt%Sb	4.055	6.14	2.6	3.7	1.07	1.63

ISSN 2347-3487

Al-15wt%Sb	4.061	6.13	3.38	4.64	1.36	2.13
Al-17wt%Sb	4.051	6.12	2.83	5.71	1.15	2.39
Al-20wt%Sb	4.054	5.88	2.95	5.55	1.21	2.35
Al-25wt%Sb	4.057	6.12	2.87	4.27	1.15	2.93
Al -33wt%Sb	4.06	6.15	2.23	7.44	0.9	3.41
Al-50wt%Sb	4.053	6.12	2.59	5.65	1.06	2.46
Al-67wt%Sb	4.05	6.04	3.01	4.57	1.26	1.86

For the AlSb phase is unmeasurably low, hinting to a good crystallization state. Lattice distortions for AlSb phase is lower than Al-12wt%Sb and for Al-67%Sb thanAl-33wt%Sb and Al-10wt%Sb table (2).This supports the optimum formation of the cubic phase. The next step after setting up and size of the unit cell is to find the number of atoms in that. From the following equation

$$\Sigma A = \frac{\rho V}{1.66020} = nA \qquad (5)$$

Where ΣA is the sum of atomic weights of the atoms in the unit cell, ρ is the density (g/cm^3), v is the volume of the unit cell, n is the number of atoms per unit cell and A the atomic weight [22]. If the substance is a chemical compound, or an intermediate phase whose composition can be represented by a simple chemical formula such as in our case aluminium antimonide(AlSb). Since the molecular weight of AlSb is 148.74, the number of atom per unit cell is 3.986, within experimental error indicated in Table 3.

Table 3: Atoms per unit cell for Al phase

System wt%	No. of atom per unit cell Al	No. of atom per unit cell AlSb
Al pure	3.7	
Al-2wt%Sb	2.8	
Al-5wt%Sb	2.64	10.1
Al-7wt%Sb	2.51	8.68
Al-10wt%Sb	3.13	10.2
Al-12wt%Sb	2.62	9.1
Al-15wt%Sb	2.6	8.99
Al-17wt%Sb	1.99	6.89
Al-20wt%Sb	2.31	7.07
Al-25wt%Sb	2.28	7.8
Al -33wt%Sb	1.41	4.93
Al-50wt%Sb	1.49	5.15
Al-67wt%Sb	1.16	3.84

The number of atoms per unit cell can be calculated from n and the composition of the phase. When determined, the number of atoms per unit cell is always an integer within experimental error, except for a few a very substances which have defect structures. In these melt – spun ribbons of Al_{100-x} - Sb_x where($x \geq$ 2wt%Sb) are simply missing from a certain fraction of those lattice sites ,which they would be excepted to occupy and the result is a nonintegral number of atoms per cell ,or some atomic sites remain vacant. This type of compound usually contains point defects and is called a nonstoichiometric compound.

ISSN 2347-3487

3.2. Surface Morphology

Fig. 5(a-m) show scanning electron Microscopy photographs of the Al_{100-x} - Sb_x where($x \geq$ 2wt%Sb) rapidly quenched ribbons by chill – block melt –spin technique at different composition. It is found that the primary AlSb uniformly distributed in the α-Al matrix in the melt –quenched ribbons. It is confirmed that the microstructure of melt –spun Al-Sb with different composition of antimony content is dominantly composed of primary AlSb particles within the α-Al solid solution matrix ,in the melt-spun alloy . It provides conclusive proof of the interconnection of the aluminium antimonide (AlSb) as non – metallic phase in each eutectic cell. This means that the two phases Al-AlSb of the Al_{100-x}-Sb_x melt quenched ribbons grow side by side into the melt. Fig(5-a,b,c,d,e,f,g,h,i,j,k,l and m) show that aluminium antimonide (AlSb) is present as a fine interconnected tangle fibers as a thread like structure and not separate globules. The results of Zhonghua Zhang et al [31] are in somewhat better agreement.

Based on the results described, the phases present in the melt-spun Al-Sb alloys were identified to the equilibrium α-Al and AlSb by XRD. Fig. 5(a-m) scanning electron Microscopy photographs of the Al_{100-x}-Sb_x where($x \geq$ 2wt%Sb)

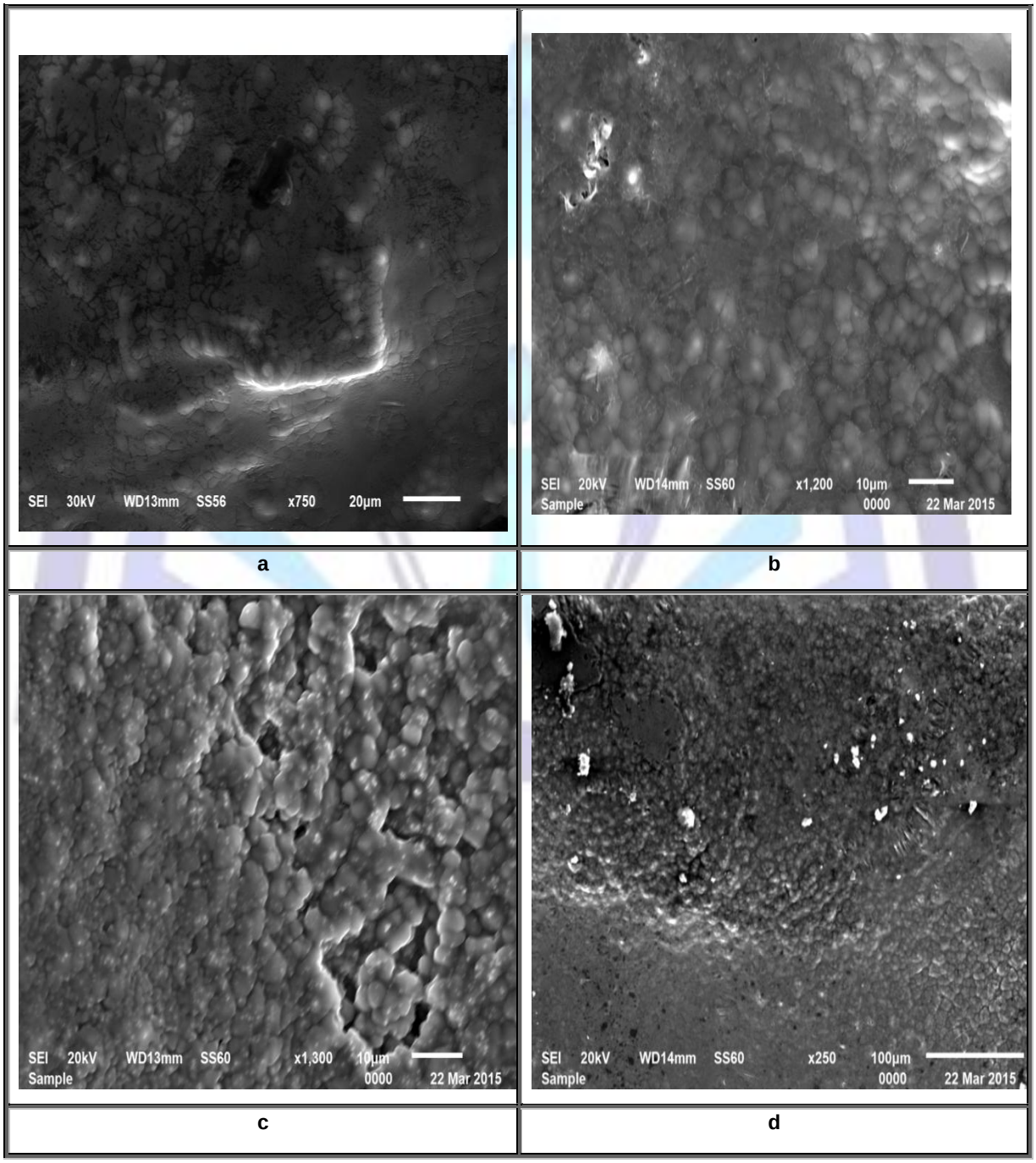

ISSN 2347-3487

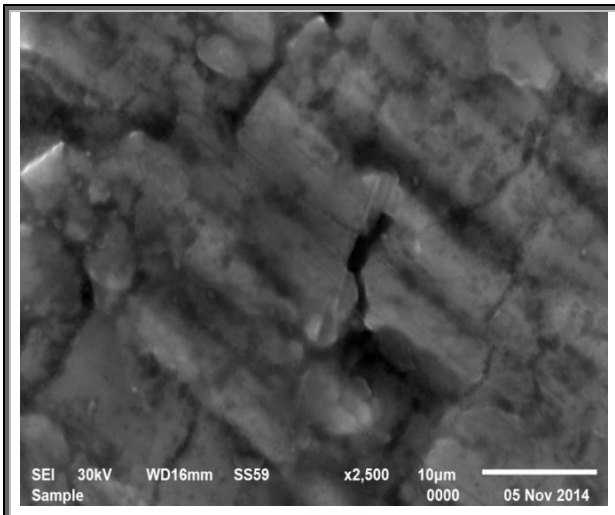

e

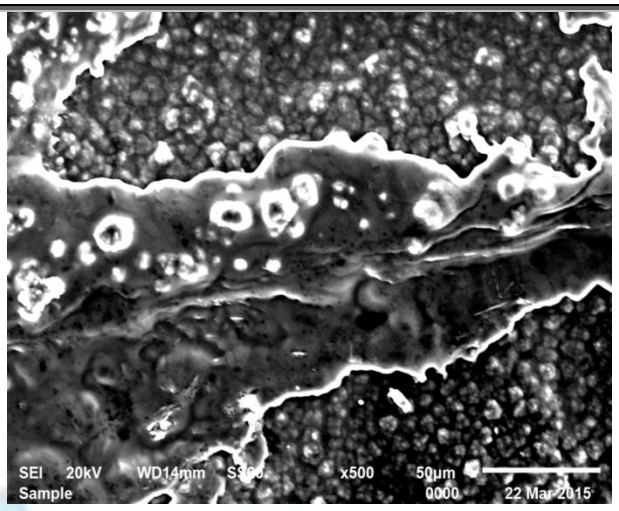

f

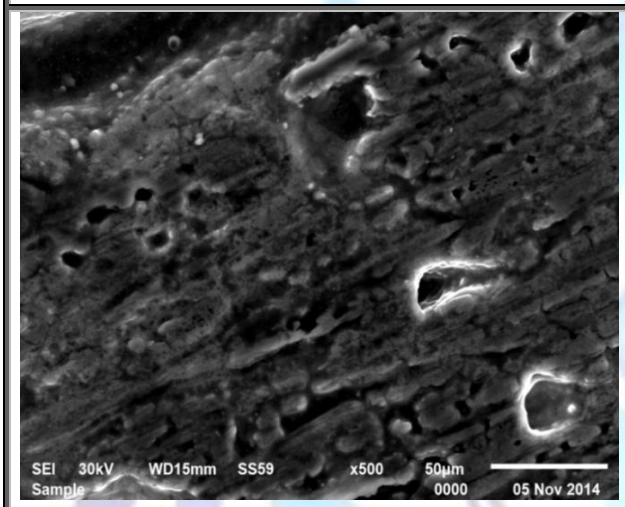

g

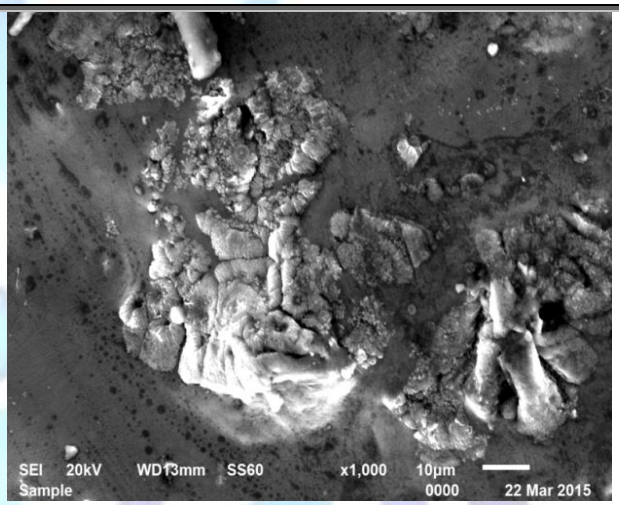

h

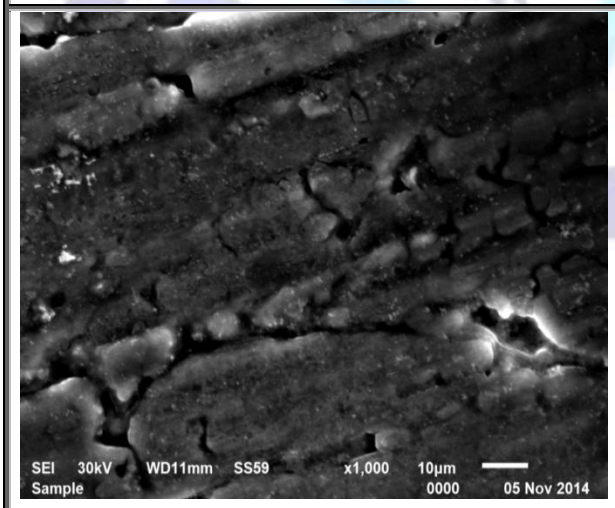

i

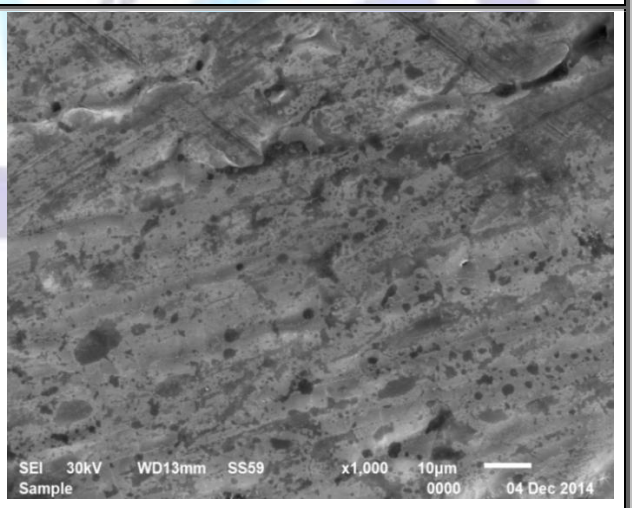

j

ISSN 2347-3487

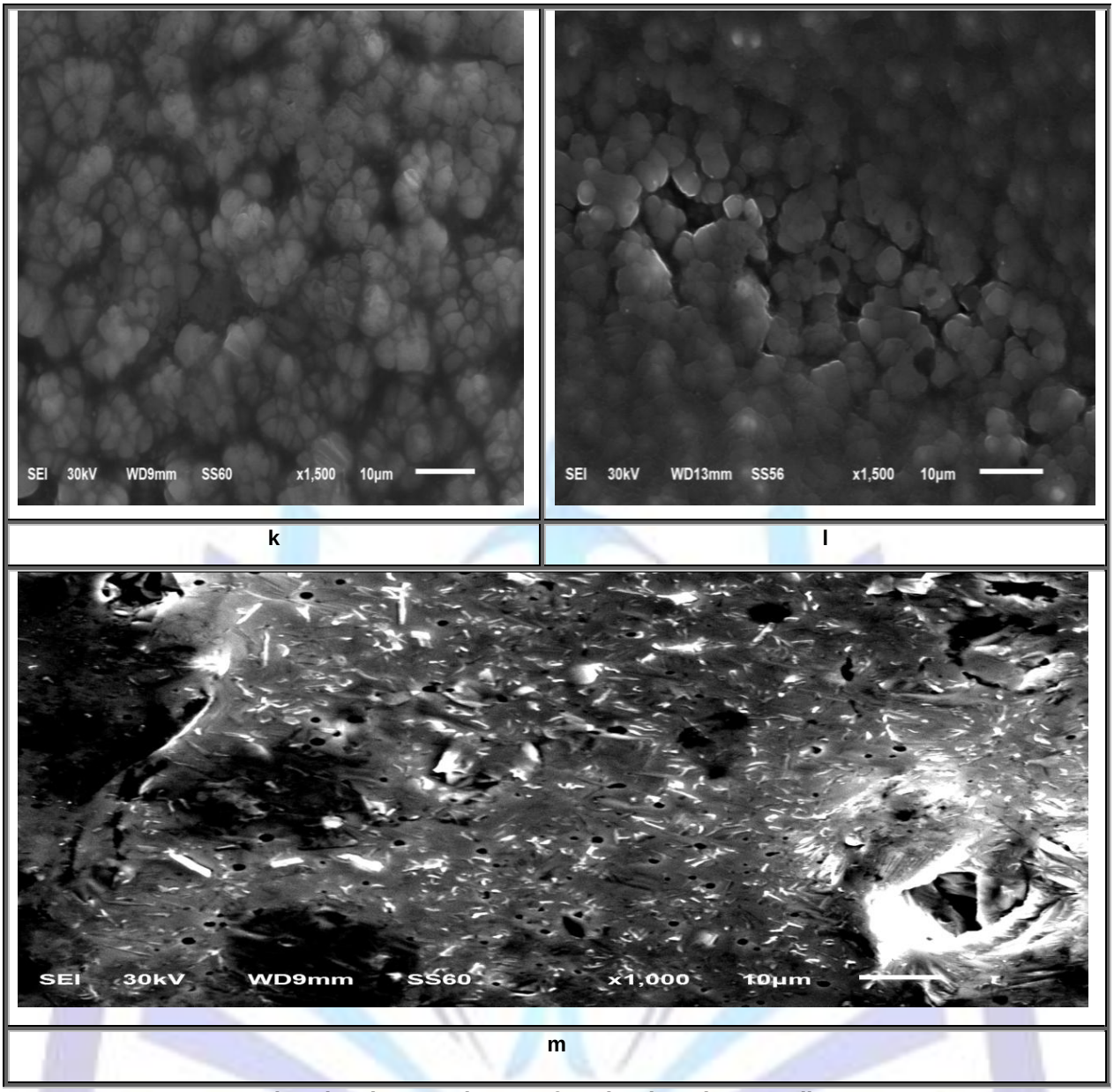

Fig.5 (a-m): SEM images for Al –Sb melt spun alloys

3.3-Resistivity data and Heat conductivity

3.3.1- Resistivity data.

The electrical resistivity behavior of the Al_{100-x} - Sb_x where ($x \geq$ 2wt%Sb) melt – quenched ribbons is well summarized by the curve represented in figure (6) corresponding to different composition : x ranging between 2wt%Sb to 67wt%Sb melt – quenched ribbons.

ISSN 2347-3487

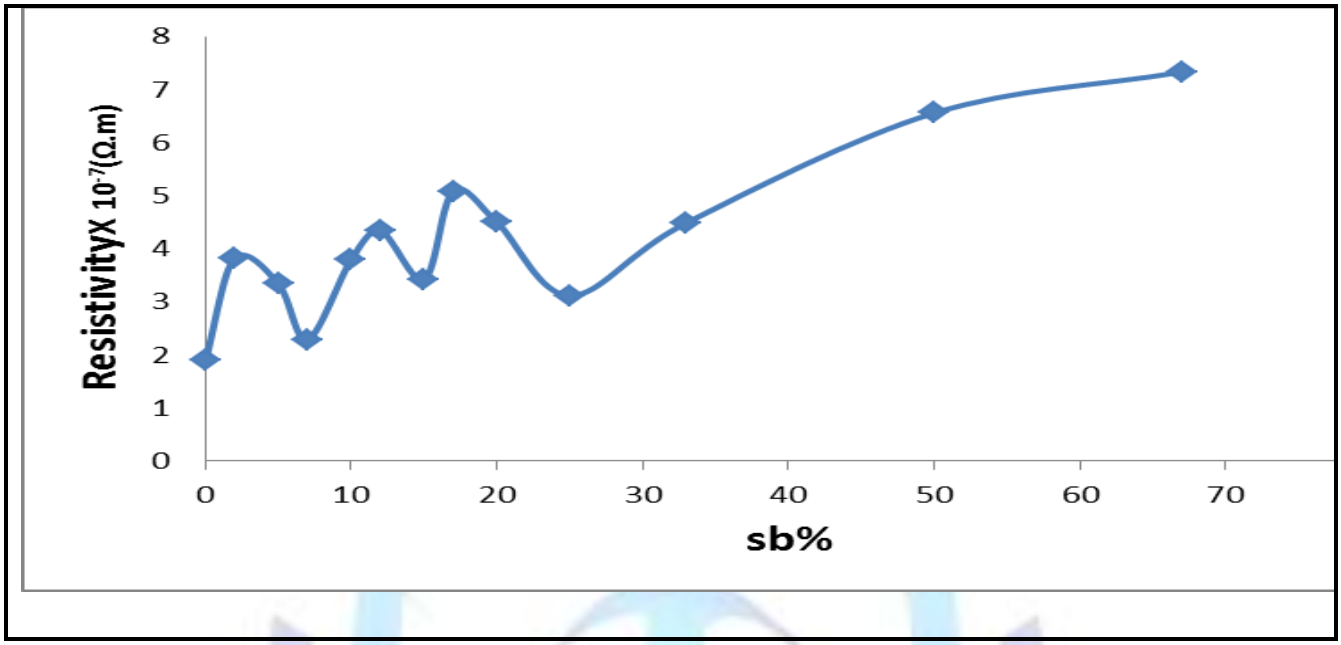

Fig.6: Electrical resistivity as a function of Sb content

Intermetallic compounds aluminium antimonide AlSb have a resistivity that is always higher than the linear values, calculated from the quantity of each constituent and the resistivity. Combining, α-Al solid solution, Sb phase and AlSb phase, we have a diagram like figure (6) for the melt –spun alloys of aluminum and antimony. From pure Al, pure Sb and pure AlSb, the curves descent rapidly for the solid solution .For aggregates of saturated solid solution , the relation is a straight line ,the resistivity depending on the amount of each crystal variety present .The maximum value of the resistivity at Al-67wt%Sb as indicated in the fig(6) and table(4). This variability of resistivity is probably due to an equilibrium condition in the alloy, for after increased addition of antimony content (beyond25wt%Sb) the resistivity increases rapidly and it was found to be in the order of $7.33x10^{-7}$ Ω .m.

Table (4): Electrical properties of Al-Sb melt spun alloys

system wt%	resistivity ρ (Ω.m) $x10^{-7}$
Al 100	1.9
Al - 2wt%Sb	3.82
Al - 5wt%Sb	3.34
Al - 7wt%Sb	2.29
Al - 10wt%Sb	3.8
Al - 12wt%Sb	4.34
Al - 15wt%Sb	3.42
Al - 17wt%Sb	5.09
Al - 20wt%Sb	4.5
Al - 25wt%Sb	3.12
Al - 33wt%Sb	4.49
Al - 50wt%Sb	6.56
Al - 67wt%Sb	7.33

ISSN 2347-3487

3.3.2. Conductivity data

The thermal conductivity changes are approximately the same way as developed for electrical resistivity. The melt – quenched ribbons of Al_{100-x} -Sb_x as shown in Fig.7 show a curve of exactly the same type was obtained for electrical resistivity of the melt – quenched ribbons of Al_{100-x} Sb_x such results to be expected on the basis that even though thermal conductivity are to be expected on the basis that even though heat conductivity is predominantly an electron function, a portion of its conductivity also arises from a direct collision of atoms.

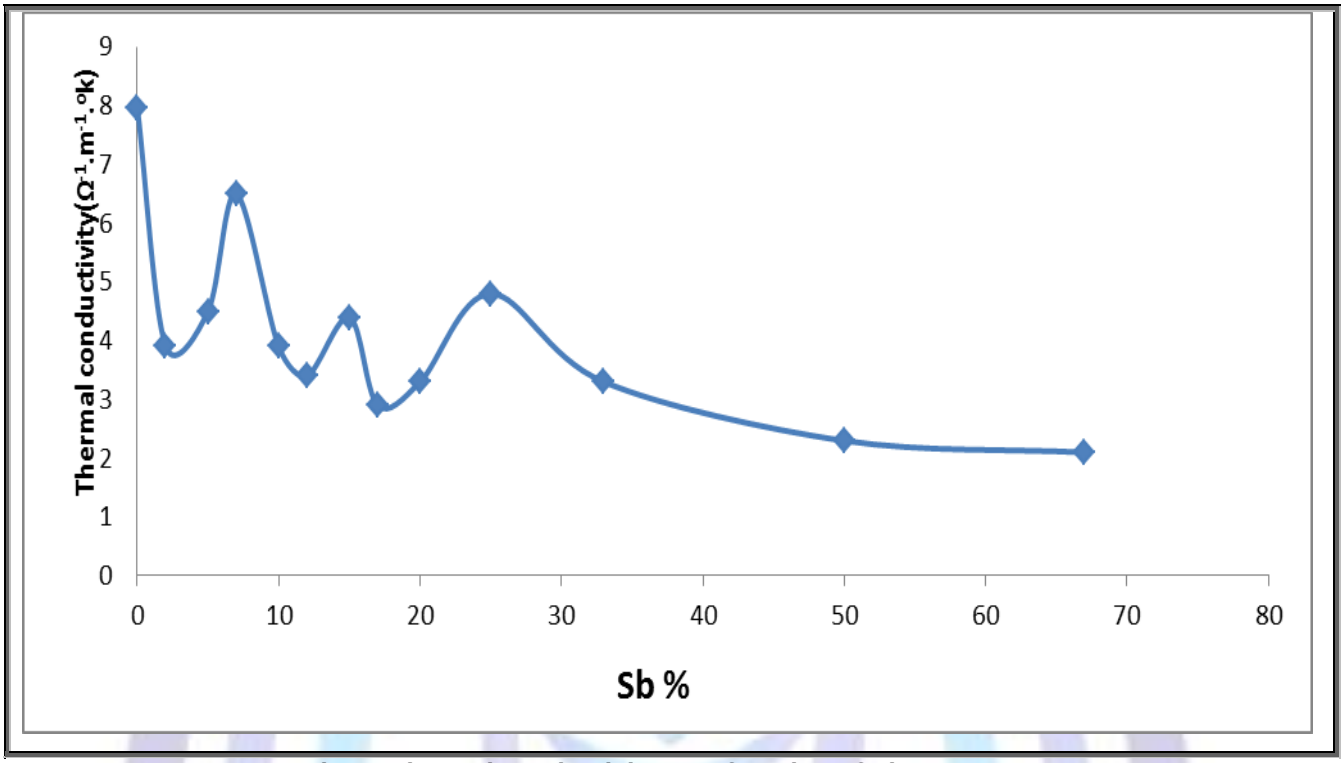

Fig.7 : Thermal conductivity as a function of Sb content

4. Elastic constants of Al_{100-x}-Sb_x melt-spun alloys:

From resonant frequencies using dynamic resonance method, the various elastic constants, such a young's modulus E, shear modulus G, bulk modulus B, and Poisson's ratio ν are calculated from the formulae

$$E=38.32\rho L^4 f^2/t^2 \quad (6)$$

$$B=\frac{E}{3(1-2\nu)} \quad (7)$$

$$G=\frac{E}{2(1+\nu)} \quad (8)$$

$$\nu = \frac{E}{2G} - 1 \quad (9)$$

Where ρ is the density of the melt –spun rapidly quenched ribbons, t is the thickness of sample and L is the length of sample. The anelasticity or internal friction of Al_{100-x}-Sb_x melt-spun ribbons Q^{-1} is calculated by equation:

$$Q^{-1}=0.5773\frac{\Delta f}{fo} \quad (10)$$

Where f is the resonance frequency of the sample .All the results are presented in table (5).the values reported are the average from the melt spun-ribbons of Al_{100-x}-$Sb_{x\,cut}$ in various directions.

ISSN 2347-3487

Table(5): Elastic constant and Internal friction Q^{-1} of Al-Sb system

System wt%	f Hz	E (Gpa)	B (Gpa)	G (Gpa)	Poisson's ritio	Δf Hz	Q^{-1} $*10^{-2}$
Al pure	57.88	66.5	73.94	24.65	0.35	1.59	1.59
Al-2wt%Sb	63.04	62.4	69.16	23.12	0.3496	1.63	1.51
Al-5wt%Sb	66.85	61.1	67.45	22.65	0.349	1.74	1.25
Al-7wt%Sb	55.26	51.7	56.88	19.16	0.3486	1.2	1.25
Al-10wt%Sb	62.66	55.2	60.48	20.46	0.348	0.8	0.74
Al-12wt%Sb	55.8	50.8	55.58	18.86	0.3476	1.23	1.27
Al-15wt%Sb	58.21	50.3	54.76	18.66	0.347	1.36	1.35
Al-17wt%Sb	61.86	48.6	52.86	18.06	0.3466	1.27	1.19
Al-20wt%Sb	63.16	45.8	49.61	17.03	0.346	0.58	0.53
Al-25wt%Sb	47.54	40.1	43.13	14.91	0.345	0.94	1.14
Al -33wt%Sb	61.99	58.3	61.9	21.7	0.343	0.97	0.9
Al-50wt%Sb	67.49	57.1	59.5	21.31	0.34	1.65	1.41
Al-67wt%Sb	69.87	46.2	47.1	17.3	0.3366	0.86	0.71

In the concentrations range of 2wt%Sb to 25wt%Sb the Young's modulus have shown a linear decrease. If can be seen that at Al-33wt%Sb show a rapid increase in the value of the Young's modulus and then decreases slowly to 46.2 Gpa .The Poisson ratio was found to be approximately constant up to Al-25wt%Sb and decreasing above this composition as indicated in table(5).

5-MicrohardnesTests

Fig.8 show the plot of microhardnes as function of antimony content for different phases formed in the melt – spun ribbons.

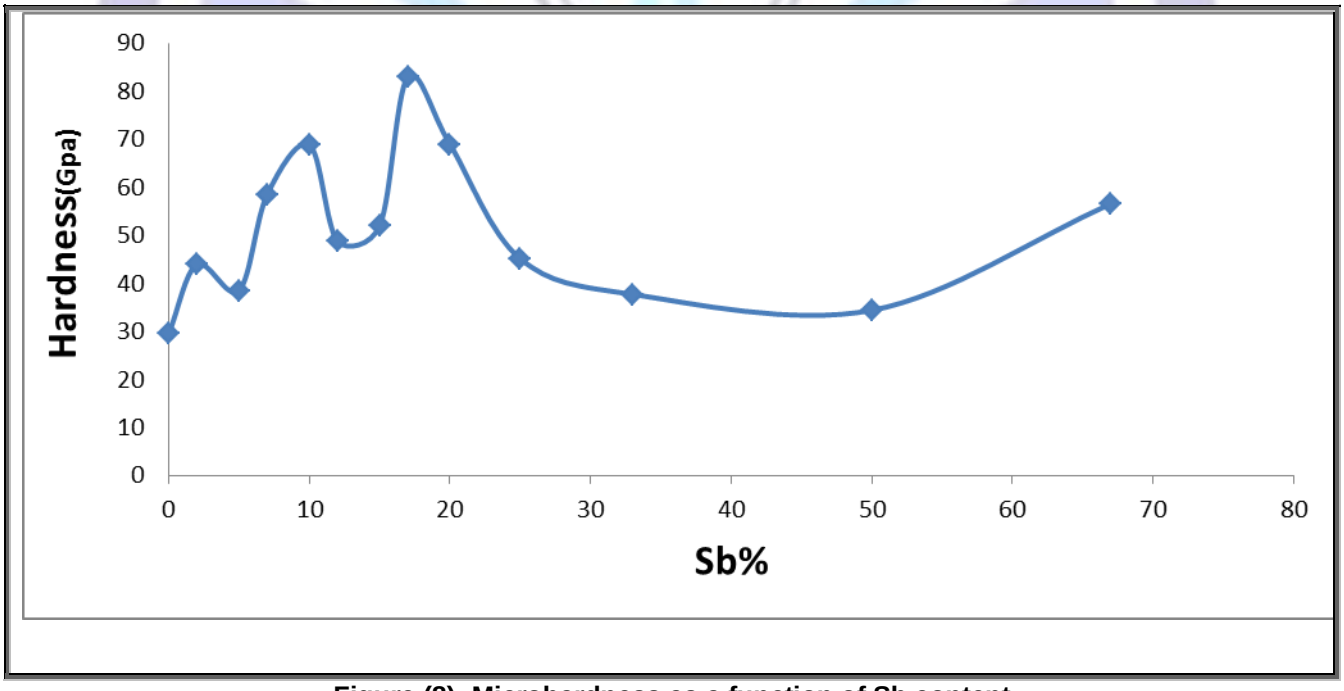

Figure (8): Microhardness as a function of Sb content

ISSN 2347-3487

The amount of aluminium antimonide (AlSb) phase in the melt –spun ribbons of Al_{100-x}-Sb_x increase with increasing antimony contents up to 20wt%Sb and then decreased up to 50wt%Sb ,but it all of a sudden increased at 67wt%Sb.We also found high hardness value for Al-17wt%Sb it is about 82.9Mpa,the may be related to AlSb rich phase in the melt –spun quenched ribbons .The microhardnes value of the melt – spun ribbons in the range between 20wt%Sb and 67wt%Sb have different values , the hardnes value of AlSb decreases with increasing antimony content. This is due the relatively low difference in bond length between Al and AlSb phase leads to an applicable solid solution non-hardening in Al-Sb alloys .This behavior may be due the diffusion and decomposition of the aluminium antimony in the melt –spun quenched ribbons Al_{100-x}-Sb_x where ($x \geq$ 2wt%Sb) alloys.

6. Conclusions

- Here we reported that the phases present in the melt-quenched ribbons Al_{100-x}-Sb_x where ($x \geq$ 2wt%Sb) alloys are α-Al and AlSb. Moreover, the lattice constant of AlSb was found to be approximately 6.088 Å with an accuracy of $\pm$ 0.062, which is in agreement with earlier published results [10, 11].

- SEM images of the melt –spun Al-Sb alloys showed that the primary AlSb uniformly distributed in an α-Al solid solution .This means that two phases grow side by side into the melt with different composition of antimony content. Therefore, rapid solidification has a great influence on the formation of aluminium antimonide (AlSb). It is obvious, that the addition of Sb has a large impact on the electrical resistivity, the resistivity maximum appears at 67wt%Sb, it was found to be in the order of (7.33×10^{-7} Ω.m). It is attributed these discontinuities to the formation of the aluminium antimonide AlSb changes in the system. -A study of variation of young modulus E , microhardens value Hv and Poisson's ratio ν (figure 9-a,b and c) and table (6) with increase of concentration of Sb in the various phases shows the values of E, Hv and ν exhibit irregular variation in the vicinity of phase transition points.

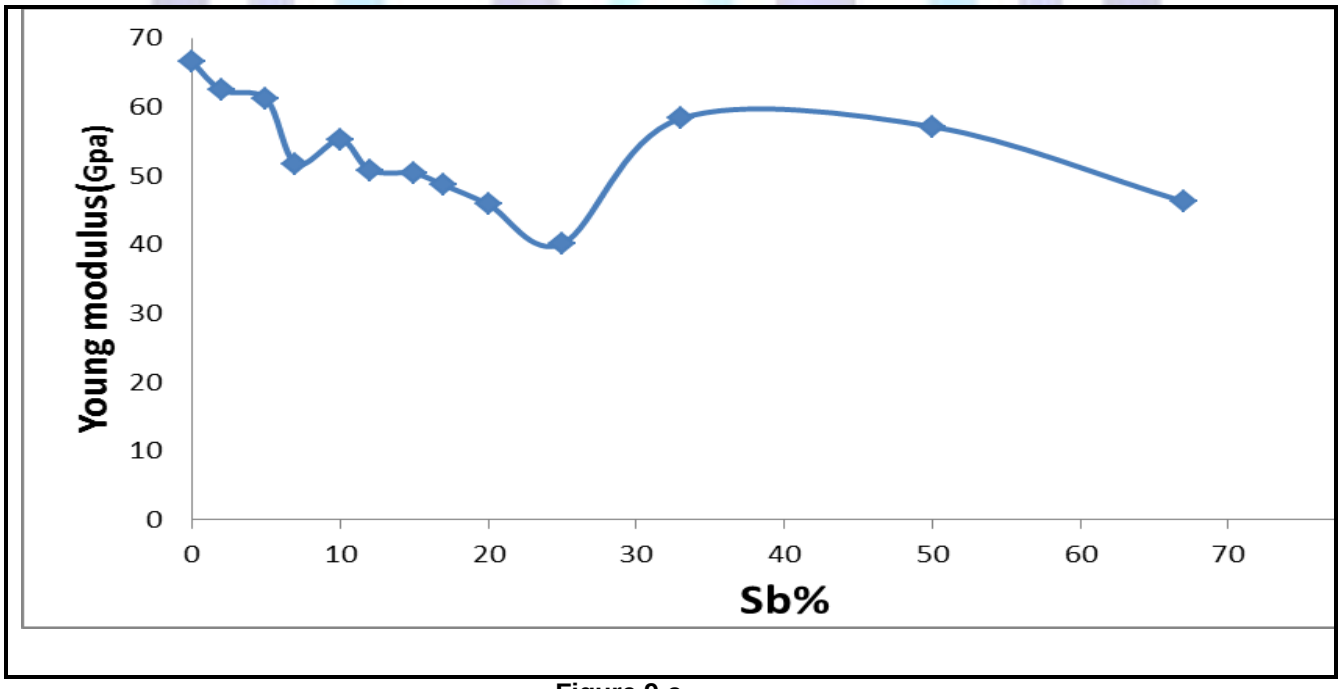

Figure 9-a

ISSN 2347-3487

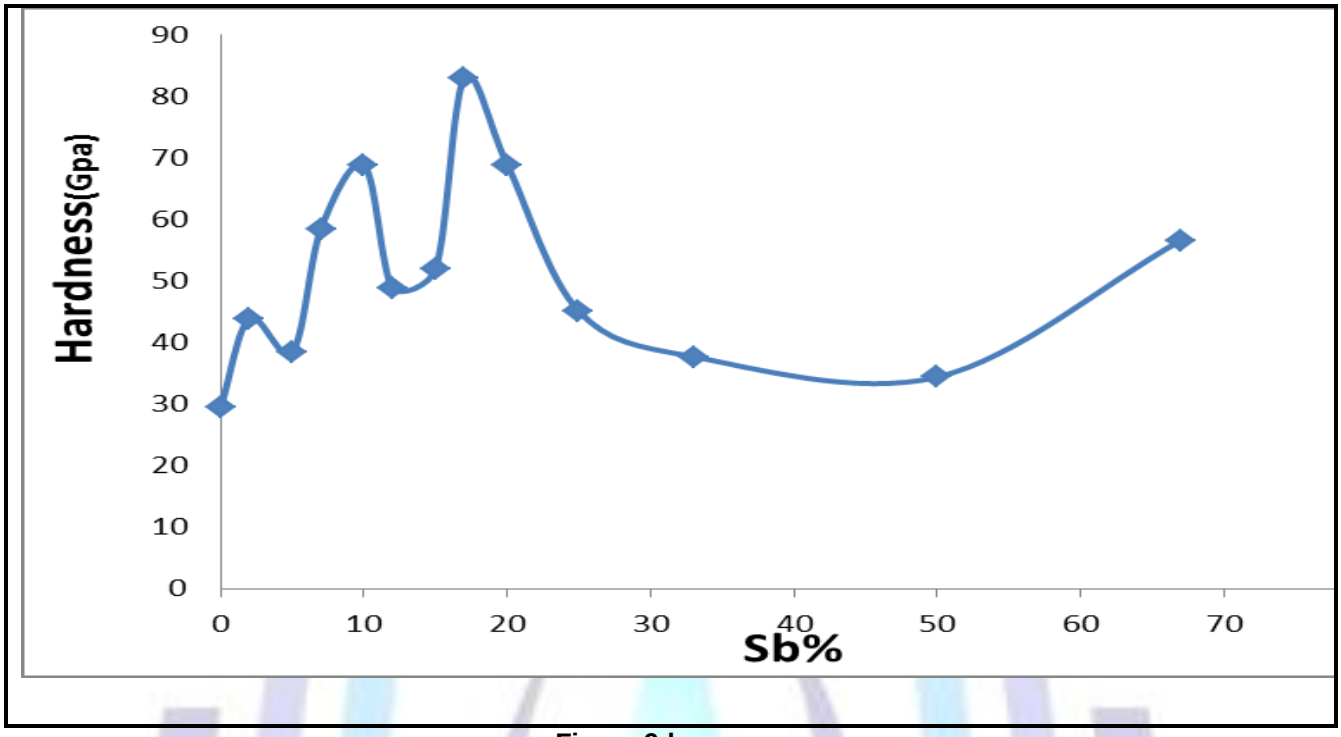

Figure 9-b

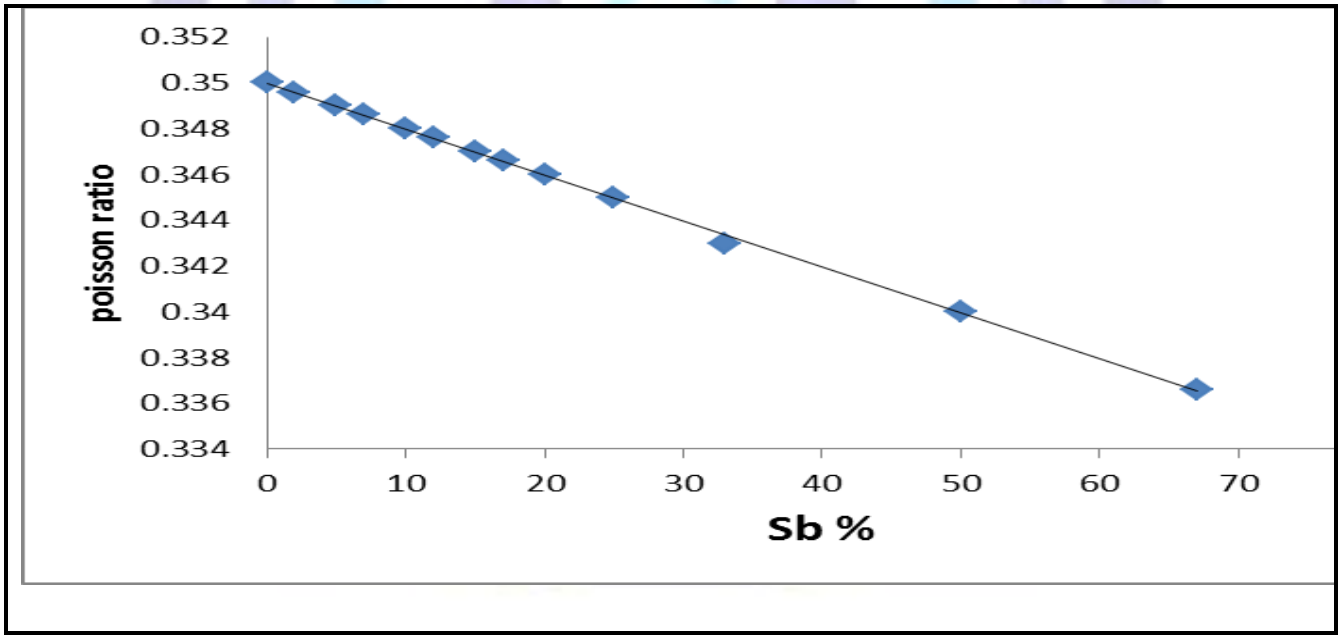

Figure 9-c

Fig 9: Young's modulus, hardness and Poisson's ratio as a function of Sb content

ISSN 2347-3487

Table 6: Mechanical properties of Al-Sb melt spun alloys

system wt%	Young modulus GPa	Hardness MPa	Poisson's ratio
Al pure	66.5	29.5	0.35
Al - 2wt%Sb	62.4	43.9	0.3496
Al - 5wt%Sb	61.1	38.5	0.349
Al - 7wt%Sb	51.7	58.5	0.3486
Al -10wt%Sb	55.2	68.8	0.348
Al -12wt%Sb	50.8	48.8	0.3476
Al -15wt%Sb	50.3	52	0.347
Al -17wt%Sb	48.6	82.9	0.3466
Al - 20wt%Sb	45.8	68.9	0.346
Al - 25wt%Sb	40.1	45.1	0.345
Al - 33wt%Sb	58.3	37.7	0.343
Al - 50wt%Sb	57.1	34.4	0.34
Al - 67wt%Sb	46.2	56.6	0.3366

- From the experimental results of the internal friction $Q^{-1,}$ it can be seen that it is more sensitive than the elastic constants to the phase changes occurring in the Al-Sb alloys

-The aluminium antimonide seems to be promising semiconducting materials for high efficiency solar material. So, further study is required to assess its peculiar properties. Other properties of the nanoscale of semiconducting compound, aluminium antimonide (AlSb) Such as electrical and thermoelectric transport properties will be investigated in details in future so that we can understand the mechanisms by which semiconducting behavior may be observed, and it finds application in the in the following Electro-optical devices, and x-ray and gamma-ray radiation .

7. References

[1] Yan Wang, Zhonghua Zhang, Shaohua, Xiufang Bian , Journal of Alloys and Compounds 370 (2004)159–163.

[2] Yan Wang , Zhonghua Zhang , Shaohua Zheng , Suhua Fan , Xin Chenga, Journal of Alloys and Compounds 376 (2004) 165–169 Weimin Wang, Xiufang Bian , Haoran Geng.

[3] Jianxiong He, Liliwu, LianghuanFeng, Jiagui Zheng, Jingquan Zhang, WeiLi , Beng Li,Yaping, Solar Energy Materials & Solar Cells 95 (2011) 369–372.

[4] L. Hsu, M. D. McCluskey, E. E. Haller, Physical Review B **67**, 035209 ~2003.

[5] H.Gautier, C.R. Hebd , Séances Acad.Sci.123,109(1896).

[6] W. Campbell and J.A. Mathews, J.A.chem .Soc.24.259(1902).

[7] C.A. Cconghanowr,U.R.Kattrer and T.Anderson CALPHAD vol.14,No.2,pp.193-202,(1990).

[8] M. Kamal, A.M.Shaban, M.El-Kady and R. Shalaby, second International conference on Engineering Mathematics and physics (ICEMP-94) Vol. 2, pp .107-121(1994) .

[9] A.M.Shaban and M.Kamal, Radiation Effects and Defects in Solids,1995 vol .133,pp ,5-13 .

[10] Tron Arne Nilsen n, Saroj Kumar Patra, Magnus Breivik, Bjørn-Ove Fimland Journal of Crystal Growth 336 (2011) 29–31.

[11] G. Giesecke , H. Pfister ,Prazisionsbestimmung der Gitterkon stanten Von AIIIBv-Verbin dungen, Acta Crystallographica 11(5) (1958)369–371.

[12]O.Madelung Semiconductors-Basic Data,Second ed .Springer,Berlin,1996.

[13] I. Vurgaftman ,J.R. Meyer, L.R.Ram, Mohan, Band parameters for III-V .Compound semiconductors and this alloy journal of Applied Physics 89(11)(2001) .

[14] 84Mca: A.J. McAlister, *Bull. Alloy Phase Diagrams,* 5(5), 462-465 (1984).

[15] Mustafa Kamal and Usama S. Mohamed, A Review: Chill-Block Melt Spin Technique, Theories & Applications, Bentham e Books, eISBN : 978-60805-151-9 , (2012) .

[16] Mustafa Kamal, Abu-Bakr El-Bediwi, Rizk Mostafa Shalaby and Mohamed Younes,Journal of Advance in physics,Vol.7,No2 (2015). 1404-1413

[17]E.Altin , E.OZ.S.Demerl, and M.Erdem, J.Mater,Sci:Mater Electron (2014)25: 5331-5337.

[18] Mustafa Kamal and Abu-Baker-El-Bediwi, Radiation, Eff. Defect solids 174(1999)211.

[19] Mustafa Kamal, Abu-Bakr El-Bediwi, and Soran Mohammed Rashid, International Journal of Engineering & Technology IJET-IJENS Vol:14 No:04,11-15.

[20] A.M. Shaban and M. Kamal, Radiation Effects and Defects in Solids, (1995),Vol.133, PP:5-13.

[21] Mustafa Kamal, Shalabia Badr and Nermin Ali Abdelhakim, International Journal of Engineering & Technology IJET-IJENS Vol: 14 No:01, pp.119-128, 2014.

[22] H. H. Liebermann, Materials Science and Engineering, 43 (1980) 203-210.

[23] C.Giacova 220,H.L.Monaco,D.Viterbo,F.Scordari,G.Gilli,G.Zanotti and M.Catti,Fundamentals of crystallography,International union of Crystallography,Oxford university press,New York,1994

[24] Mustafa Kamal, Abu-Bakr El-Bediwi and Samira El-Mohamady Fouda , International Journal of Engineering & Technology IJET-IJENS ,Vol.13 ,No:06 PP:29-38 .

[25] T.Gandhi,K.S.Raija,M.Misra,Electrochimica Acta,53(2008) 7331-7337

[26] Akram Hashim Taha, American Journal of Condensed Matter Physics 2014, 4(4): 63-70.

[27] Y. R. Toda, K. S. Chaudhari, A. B. Jain, D. N. Gujarathi, Scholars Research Library, Archives of Physics Research, 2011, 2 (1): 146-153

[28] W. H. Hall and G. K. Willamson, Proc. Phys. Soc. 64 B (1951) 937-946.

[29] G. K. Williason and W.H. Hall, Acta Metallurgical, Vol .1, Jan.(1953) 22-31.

[30]I,Lucks,P.Lamparter and E.J. Mittemeijer,J. Appl,Cryst.(2004),37,300-311.

[31] Zhonghua Zhang , Xiufang Bian , Yan Wang , Journal of alloys and Compounds 351(2003) 184-189.